Available online at www.sciencedirect.com
ScienceDirect
Advances in Water Resources 31 (2008) 383–398
Advances in Water Resources
www.elsevier.com/locate/advwatres

# Effect of wellbore storage and finite thickness skin on flow to a partially penetrating well in a phreatic aquifer

M. Pasandi [a], N. Samani [a,*], D.A. Barry [b,1]

[a] Department of Earth Sciences, College of Sciences, Shiraz University, Shiraz 71454, Iran
[b] Laboratoire de technologie écologique, Institut des sciences et technologies de l'environnement, Station No. 2, Ecole Polytechnique Fédérale de Lausanne, CH-1015 Lausanne, Switzerland

Received 1 June 2007; received in revised form 17 September 2007; accepted 19 September 2007
Available online 25 September 2007

**Abstract**

An analytical model is presented for the analysis of constant flux tests conducted in a phreatic aquifer having a partially penetrating well with a finite thickness skin. The solution is derived in the Laplace transform domain for the drawdown in the pumping well, skin and formation regions. The time-domain solution in terms of the aquifer drawdown is then obtained from the numerical inversion of the Laplace transform and presented as dimensionless drawdown–time curves. The derived solution is used to investigate the effects of the hydraulic conductivity contrast between the skin and formation, in addition to wellbore storage, skin thickness, delayed yield, partial penetration and distance to the observation well. The results of the developed solution were compared with those from an existing solution for the case of an infinitesimally thin skin. The latter solution can never approximate that for the developed finite skin. Dimensionless drawdown–time curves were compared with the other published results for a confined aquifer. Positive skin effects are reflected in the early time and disappear in the intermediate and late time aquifer responses. But in the case of negative skin this is reversed and the negative skin also tends to disguise the wellbore storage effect. A thick negative skin lowers the overall drawdown in the aquifer and leads to more persistent delayed drainage. Partial penetration increases the drawdown in the case of a positive skin; however its effect is masked by the negative skin. The influence of a negative skin is pronounced over a broad range of radial distances. At distant observation points the influence of a positive skin is too small to be reflected in early and intermediate time pumping test data and consequently the type curve takes its asymptotic form.


*Keywords:* Ground water; Analytical solution; Pumping test; Unsteady flow; Laplace transform

## 1. Introduction

Pumping tests remain the standard method to evaluate the hydrodynamic properties of subsurface material for water-supply purposes. Aquifer response data from a pumping test can be employed to estimate subsurface properties using schemes based on analytical or numerical solutions to the appropriate flow conditions. This methodology is founded on a series of assumptions required to reduce the complex natural system to a mathematically tractable one. The estimated hydraulic parameters can be erroneous if the configuration of the aquifer and the well is different from the one assumed.

Traditionally, pumping test analysis has been limited to applications involving aquifers whose properties are assumed uniform in space. For example, wellbore storage acts to delay the transmission of fluid from the formation to the well. By ignoring wellbore storage and using the line-source approximation to analyze the results of an aquifer test, values of $T$ will be underestimated and values of $S$ will be overestimated (symbol definitions are given in Nomenclature).

* Corresponding author. Tel.: +98 711 228 2380; fax: +98 711 228 0926.
*E-mail addresses:* Pasandi@susc.ac.ir (M. Pasandi), Samani@susc.ac.ir (N. Samani), andrew.barry@epfl.ch (D.A. Barry).
[1] Tel.: +41 21 693 5576; fax: +41 21 693 5670.

0309-1708/$ - see front matter © 2007 Elsevier Ltd. All rights reserved.
doi:10.1016/j.advwatres.2007.09.001

**Nomenclature**

| | |
|---|---|
| $r$ | radial distance from the axis of pumping well, L |
| $r_w$ | radius of the well, L |
| $r_c$ | inside radius of the pumped well over the range of changing water levels during pumpage, L |
| $r_s$ | radius of the skin, L |
| $z$ | vertical distance above the bottom, L |
| $b$ | initial saturated thickness of aquifer, L |
| $d$ | vertical distance from initial water table to top of well screen, L |
| $l$ | vertical distance from initial water table to bottom of well screen, L |
| $s_1$ | drawdown in the skin region, L |
| $s_2$ | drawdown in the formation region, L |
| $s_w$ | drawdown in the pumping well, L |
| $t$ | time since start of pumping, T |
| $Q$ | pumping rate, $L^3\,T^{-1}$ |
| $K_{r1}, K_{r2}$ | hydraulic conductivity in the horizontal direction, $L\,T^{-1}$ |
| $K_{z1}, K_{z2}$ | hydraulic conductivity in the vertical direction, $L\,T^{-1}$ |
| $S_{y1}, S_{y2}$ | specific yield |
| $S_{s1}, S_{s2}$ | specific storage, $L^{-1}$ |
| $C_{s1} = \frac{K_{r1}}{S_{s1}}, C_{s2} = \frac{K_{r2}}{S_{s2}}$ | Hydraulic diffusivity, $L^2\,T^{-1}$ |
| $\alpha_1, \alpha_2$ | empirical constant describing the drainage from the unsaturated zone, $T^{-1}$ |
| $P$ | Laplace transform variable |
| $I_0(\cdot), K_0(\cdot), I_1(\cdot), K_1(\cdot)$ | Modified Bessel functions |
| $\gamma$ | Euler's constant (0.5772) |

*Subscripts*

| | |
|---|---|
| 1,2 | skin zone, formation |

Wellbore damage or improvement also influences the results of interwell hydraulic tests. The term skin effect is used to describe the damage or improvement to the region surrounding the well that is caused by drilling practices. Wellbore skin effects can be examined mathematically in two ways: (1) by assuming the skin to be infinitesimally thin, and (2) by assuming it to be of finite thickness [8]. The effect of both wellbore storage and the skin region on the results of pumping tests has long been investigated in the petroleum industry [10,24,28] and in groundwater studies [5,13,19–22,25,27]. These solutions account for wellbore storage and an infinitesimally thin skin in both pumping and observation wells. The concept of an infinitesimally thin skin is in certain circumstances realistic as well as being a mathematically convenient means of linking the hydraulic head in the formation to the hydraulic head in the borehole. In such cases, the skin is assumed to have no storativity. This assumption permits an estimate of the skin factor if the storage coefficient of the formation is known. The effects of the infinitesimal skin tend to be indistinguishable from the effects of a decrease in the storage coefficient in the analytical solution [14].

Clearly, a more versatile treatment of wellbore skin effects is achieved using composite analytical models in which the skin region, like the formation region, has a finite thickness, permeability and storativity. This type of composite model was used by numerous authors [2,4,6,11,12,14,17,18,29–33] for the analysis of confined aquifers.

Perina and Lee [23] have presented a general well function for groundwater flow toward an extraction well partially penetrating a confined, leaky or unconfined aquifer. They have taken a non-uniform radial flux along the screen and a finite-thickness skin into account but they did not analyze wellbore storage and finite-thickness skin effects on the flow to these kinds of aquifers. Moreover, they assumed that drainage from the zone above the water table occurs instantaneously in response to a decline in the elevation of the water table [16]. Moench [15] presented a Laplace transform solution for the problem of flow to a partially penetrating well of finite diameter in a slightly compressible phreatic aquifer. This solution allows the evaluation of both pumped well and observation piezometer data. It accounts for effects of wellbore storage and a thin skin and also takes into account the non-instantaneous and instantaneous release of water from the unsaturated zone. Because the skin region is usually of finite thickness, development of a model is necessary for the problem of a phreatic aquifer in which the medium is represented by two regions of radial flow each with individual hydrodynamic properties and thickness.

The following mathematical development is for the flow to a partially penetrating well in a phreatic aquifer where the influence of wellbore storage and a skin region of finite thickness are present. This model is similar to the solution by Moench [15], with the exception of the finite thickness skin. The solution is obtained in Laplace space and inverted numerically using the Stehfest method [26]. This solution can be used to investigate the effects of skin type, skin thickness, wellbore storage, partial penetration, non-instantaneous and instantaneous release of water from the unsaturated zone and distance to the observation point on the drawdown distribution in a radial two-region phreatic aquifer flow system. The major purpose of this paper is to demonstrate how this solution can be used to develop insight into pumping-induced flow in non-uniform aquifers. In other words, the emphasis is on the development of insight into how aquifer and well characteristics affect pumping-induced drawdown, so that field practitioners will have a better idea of what to expect when working in natural systems. A comparison to the case of infinitesimally thin skin [15] is made and the influence of the finite thick-

ness skin and its parameters on the results of pumping tests will also be investigated.

## 2. Analytical solution

The assumptions regarding the well and aquifer configurations for a radial two-region phreatic aquifer system as shown in Fig. 1 are [7,15,16]: (1) the aquifer is homogeneous and anisotropic, of infinite lateral extent, and with uniform thickness horizontally. (2) Vertical flow across the lower boundary of the aquifer is negligible. (3) The well discharges at a constant rate from a specified zone below an initially horizontal water table. (4) The head within the well does not vary spatially. (5) The radial flux from the aquifer to the well does not vary along the length of the screened section [9]. (6) The vertical flux from the aquifer through the base of the well is negligible. (7) The porous medium and fluid are slightly compressible and have constant physical properties. (8) The initial hydraulic head is spatially uniform. (9) The finite radius well is partially penetrating (10) In addition to the instantaneous elastic response of aquifer compression and water expansion, gravity drainage of the pores is considered. (11) The drawdown is considered small compared with the saturated thickness so that boundary conditions appropriate for an initially horizontal water table can be imposed. (12) It is also assumed that the vertical flux of water into the aquifer from the unsaturated zone occurs in a manner that varies exponentially with time in response to a step decline in hydraulic head at the water table.

Under these assumptions the governing equations for the skin and formation regions are given in dimensional format as, respectively,

$$\frac{\partial^2 s_1}{\partial r^2}+\frac{1}{r}\frac{\partial s_1}{\partial r}+K_{D1}\frac{\partial^2 s_1}{\partial z^2}=\frac{1}{C_{s1}}\frac{\partial s_1}{\partial t},\quad r_w\leqslant r\leqslant r_s, \tag{1}$$

and

$$\frac{\partial^2 s_2}{\partial r^2}+\frac{1}{r}\frac{\partial s_2}{\partial r}+K_{D2}\frac{\partial^2 s_2}{\partial z^2}=\frac{1}{C_{s2}}\frac{\partial s_2}{\partial t},\quad r\geqslant r_s, \tag{2}$$

where the subscripts 1 and 2, respectively, denote the skin and formation regions; $s$ is drawdown [L]; $r$ is radial distance from the well centerline [L]; $r_w$ is well radius [L]; $r_s$ is radial distance from the well centerline to the outer skin boundary [L]; $t$ is time since the start of pumping [T]; $K_{D1}=\frac{K_{z1}}{K_{r1}}$, $K_{D2}=\frac{K_{z2}}{K_{r2}}$, $C_{s1}=\frac{K_{r1}}{S_{s1}}$ and $C_{s2}=\frac{K_{r2}}{S_{s2}}$ where $K_r$ and $K_z$ are the hydraulic conductivity in horizontal and vertical plane, respectively [L $T^{-1}$] and $S_s$ is specific storage [$L^{-1}$].

The phreatic surface is initially horizontal, with zero drawdown in both the skin and the formation,

$$s_1(r,z,0)=s_2(r,z,0)=0, \tag{3}$$

with the same condition for the drawdown in the well:

$$s_w(r_w,z,0)=0. \tag{4}$$

The head at infinity is fixed, so the boundary condition for the formation zone is:

$$s_2(\infty,z,t)=0. \tag{5}$$

The boundary condition representing the extension of the casing is [15]:

$$\left.\frac{\partial s_1}{\partial r}\right|_{r=r_w}=0,\quad z<b-l,\quad z>b-d, \tag{6}$$

where $z$, $b$, $l$ and $d$ are shown in Fig. 1. The continuity equation at the well face is approximated as [7,15]:

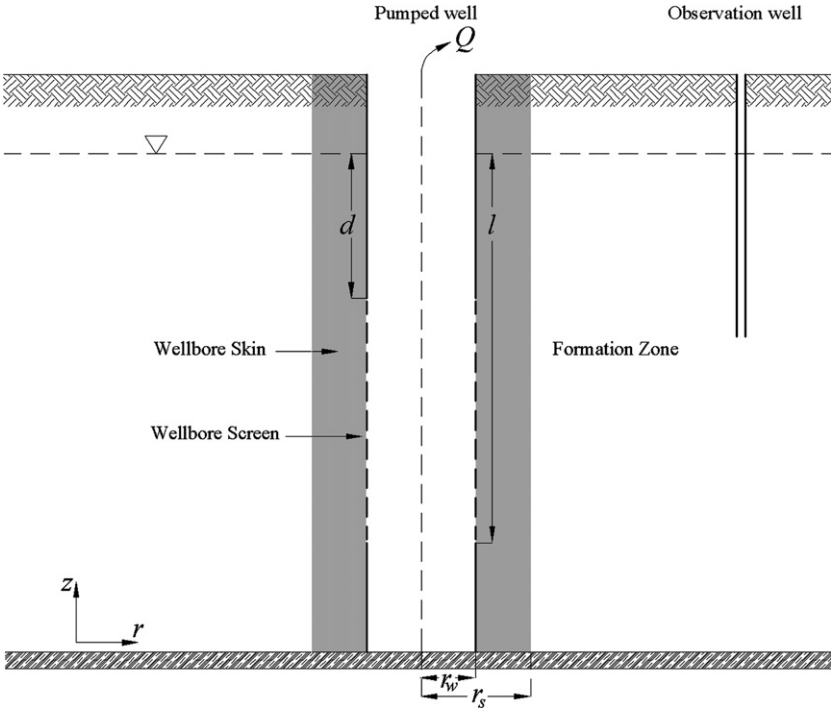


Fig. 1. Schematic diagram of the well and the aquifer.

$$2\pi r_w(l-d)K_{r1}\left.\frac{\partial s_1}{\partial r}\right|_{r=r_w} = C\frac{ds_w}{dt} - Q, \quad b-l \leqslant z \leqslant b-d, \tag{7}$$

where $l-d$ is the length of the screen, $C$ is the wellbore storage coefficient [$L^2$], which accounts for the wellbore storage capacity, equal to $\pi r_c^2$ for open wells ($r_c$ is the radius of the standpipe in the interval where water levels are changing; $r_c$ may be different to the radius of the well). In this case, $C$ is the cross-sectional area of the free surface in the well. The fluid compressibility is neglected in the wellbore accumulation terms because volume changes due to liquid level dominate. The radial flow from the aquifer to the well at the sand face is assumed to be independent of vertical coordinate $z$ and varies only with time [7,15]. $Q$ is the constant discharge rate [$L^3\,T^{-1}$], $s_w$ is the average drawdown in the wellbore. The no-flow boundary conditions at the bottom impervious boundary are:

$$\left.\frac{\partial s_1}{\partial z}\right|_{z=0} = \left.\frac{\partial s_2}{\partial z}\right|_{z=0} = 0. \tag{8}$$

The conditions at the water table, which approximate the rate of drainage per unit area from the unsaturated zones of the two regions, are [15]:

$$K_{z1}\left.\frac{\partial s_1}{\partial z}\right|_{z=b} = -\alpha_1 S_{y1}\int_0^t \frac{\partial s_1}{\partial t'}e^{-\alpha_1(t-t')}\,dt', \quad r_w \leqslant r \leqslant r_s \quad \text{and} \tag{9}$$

$$K_{z2}\left.\frac{\partial s_2}{\partial z}\right|_{z=b} = -\alpha_2 S_{y2}\int_0^t \frac{\partial s_2}{\partial t'}e^{-\alpha_2(t-t')}\,dt', \quad r \geqslant r_s. \tag{10}$$

The rate of exponential decline in the skin and formation regions is controlled by empirical relaxation coefficients $\alpha_1$ and $\alpha_2$, respectively [1,15,22]. $S_{y1}$ and $S_{y2}$ are specific yields pertaining to the two regions.

In order to ensure continuity of flow between the skin region and the undisturbed formation, auxiliary conditions at the skin-formation boundary $r_s$ must also be met. Continuity between the well and the skin region is given by:

$$s_w(r_w,z,t) = s_1(r_w,z,t). \tag{11}$$

The drawdown is continuous at the interface between the skin zone and the undisturbed formation:

$$s_1(r_s,z,t) = s_2(r_s,z,t), \tag{12}$$

while there is also conservation of flux at this interface:

$$K_{r1}\frac{\partial s_1(r_s,z,t)}{\partial r} = K_{r2}\frac{\partial s_2(r_s,z,t)}{\partial r}. \tag{13}$$

A solution to (1) and (2) with respect to the conditions (3)–(13) can be found in the Laplace transform domain. Details of the solution are given in the Appendix. The results for the dimensionless drawdowns in the Laplace domain for a partially penetrating well configuration are expressed as

$$\bar{s}_{D1} = \sum_{n=0}^{\infty}\frac{\zeta_1[K_0(q_{n1}r_D)\psi_1 + I_0(q_{n1}r_D)\psi_2]}{C_D P K_{rR}[I_0(q_{n1})\psi_1 + C_D P K_0(q_{n1})\psi_2][2\cos(\varepsilon_{n1})\delta_2 + \delta_1\varepsilon_{n1}(d_D-l_D)] + q_{n1}\zeta_2[K_1(q_{n1})\psi_1 - q_{n1}I_1(q_{n1})\psi_2]}, \tag{14}$$

$$\bar{s}_{D2} = \sum_{n=0}^{\infty}\frac{q_1 K_0(q_{n2}r_D)\zeta_1[K_0(q_{n1}r_{sD})I_1(q_{n1}r_{sD}) + I_0(q_{n1}r_{sD})K_1(q_{n1}r_{sD})]}{C_D P K_{rR}[I_0(q_{n1})\psi_1 + C_D P K_0(q_{n1})\psi_2][2\cos(\varepsilon_{n1})\delta_2 + \delta_1\varepsilon_{n1}(d_D-l_D)] + q_{n1}\zeta_2[K_1(q_{n1})\psi_1 - q_{n1}I_1(q_{n1})\psi_2]} \tag{15}$$

and

$$\bar{s}_{wD} = \sum_{n=0}^{\infty}\frac{\zeta_1[K_0(q_{n1}r_{wD})\psi_1 + I_0(q_{n1}r_{wD})\psi_2]}{C_D P K_{rR}[I_0(q_{n1})\psi_1 + C_D P K_0(q_{n1})\psi_2][2\cos(\varepsilon_{n1})\delta_2 + \delta_1\varepsilon_{n1}(d_D-l_D)] + q_{n1}\zeta_2[K_1(q_{n1})\psi_1 - q_{n1}I_1(q_{n1})\psi_2]}, \tag{16}$$

where $P$ is the Laplace variable, $\bar{s}_{D1}$, $\bar{s}_{D2}$ and $\bar{s}_{wD}$ are the Laplace-domain solutions for the skin region, formation region and the pumping well, respectively (all dimensionless parameters in above and proceeding equations are defined in Table 1) and

Table 1
Dimensionless variables

| | |
|---|---|
| $r_D$ | $r/r_w$ |
| $r_{wD}$ | $r_w/b$ |
| $r_{sD}$ | $r_s/r_w$ |
| $z_D$ | $\frac{z}{b}$ |
| $d_D$ | $\frac{d}{b}$ |
| $l_D$ | $\frac{l}{b}$ |
| $s_{D1}$ | $\frac{4\pi b K_{r2} s_1}{Q}$ |
| $s_{D2}$ | $\frac{4\pi b K_{r2} s_2}{Q}$ |
| $s_{wD}$ | $\frac{4\pi b K_{r2} s_w}{Q}$ |
| $t_D$ | $\frac{tC_{s2}}{r_w^2}$ |
| $K_{D1}$ | $\frac{K_{z1}}{K_{r1}}$ |
| $K_{D2}$ | $\frac{K_{z2}}{K_{r2}}$ |
| $C_{sR}$ | $\frac{C_{s2}}{C_{s1}}$ |
| $K_{rR}$,$K_{zR}$ | $\frac{K_{r2}}{K_{r1}}$, $\frac{K_{z2}}{K_{z1}}$ |
| $C_D$ | $\frac{C}{2\pi r_w^2(l-d)S_{s2}}$ |
| $\gamma_1$ | $\frac{\alpha_1 b S_{y1}}{K_{z1}}$ |
| $\gamma_2$ | $\frac{\alpha_2 b S_{y2}}{K_{z2}}$ |
| $\beta_{w1}$ | $K_{D1}r_{wD}^2$ |
| $\beta_{w2}$ | $K_{D2}r_{wD}^2$ |
| $\beta_1$ | $\beta_{w1}r_D^2$ |
| $\beta_2$ | $\beta_{w2}r_D^2$ |
| $\sigma_1$ | $\frac{S_{s1}b}{S_{y1}}$ |
| $\sigma_2$ | $\frac{S_{s2}b}{S_{y2}}$ |

$$\zeta_1 = -4K_{rR}\cos(\varepsilon_{n1}z_D)\{\cos(\varepsilon_{n1})[\sin(\varepsilon_{n1}d_D) - \sin(\varepsilon_{n1}l_D)] - \sin(\varepsilon_{n1})[\cos(\varepsilon_{n1}l_D) - \cos(\varepsilon_{n1}d_D)]\}/P(d_D - l_D), \quad (17)$$

$$\zeta_2 = \varepsilon_{n1} + \sin(\varepsilon_{n1})\cos(\varepsilon_{n1}), \quad (18)$$

$$\psi_1 = q_{n1}K_0(q_{n2}r_{sD})I_1(q_{n1}r_{sD}) - K_{rR}q_{n2}K_1(q_{n2}r_{sD})I_0(q_{n1}r_{sD}), \quad (19)$$

$$\psi_2 = q_{n1}K_0(q_{n2}r_{sD})K_1(q_{n1}r_{sD}) - K_{rR}q_{n2}K_1(q_{n2}r_{sD})K_0(q_{n1}r_{sD}), \quad (20)$$

$$\delta_1 = [\sin(2\varepsilon_{n1}d_D) - \sin(2\varepsilon_{n1}l_D)]/2 \quad \text{and} \quad (21)$$

$$\delta_2 = \sin(\varepsilon_{n1})\left[\frac{\cos(2\varepsilon_{n1}d_D) - \cos(2\varepsilon_{n1}l_D)}{2}\right] + \cos(\varepsilon_{n1})\left[\frac{\sin(2\varepsilon_{n1}l_D) - \sin(2\varepsilon_{n1}d_D)}{2}\right]. \quad (22)$$

For a fully penetrating well the foregoing equations reduce to:

$$\bar{s}_{D1} = \sum_{n=0}^{\infty} \frac{4K_{rR}\sin(\varepsilon_{n1})\cos(\varepsilon_{n1}z_D)[K_0(q_{n1}r_D)\psi_1 + I_0(q_{n1}r_D)\psi_2]}{P\zeta_2[\xi_2\psi_2 - \xi_1\psi_1]}, \quad (23)$$

$$\bar{s}_{D2} = \sum_{n=0}^{\infty} \frac{-4K_{rR}q_{n1}\sin(\varepsilon_{n1})\cos(\varepsilon_{n1}z_D)K_0(q_{n2}r_D)[K_0(q_{n1}r_{sD})I_1(q_{n1}r_{sD}) + I_0(q_{n1}r_{sD})K_1(q_{n1}r_{sD})]}{P\zeta_2[\xi_2\psi_2 - \xi_1\psi_1]} \quad (24)$$

and

$$\bar{s}_{wD} = \sum_{n=0}^{\infty} \frac{4K_{rR}\sin(\varepsilon_{n1})\cos(\varepsilon_{n1}z_D)[K_0(q_{n1}r_{wD})\psi_1 + I_0(q_{n1}r_{wD})\psi_2]}{P\zeta_2[\xi_2\psi_2 - \xi_1\psi_1]}, \quad (25)$$

where

$$\xi_1 = q_{n1}K_1(q_{n1}) + C_DPK_{rR}K_0(q_{n1}), \quad (26)$$

$$\xi_2 = q_{n1}I_1(q_{n1}) - C_DPK_{rR}I_0(q_{n1}), \quad (27)$$

$$q_{n1} = (\beta_{w1}\varepsilon_{n1}^2 + C_{sR}P)^{1/2} \quad \text{and} \quad (28)$$

$$q_{n2} = (\beta_{w2}\varepsilon_{n2}^2 + P)^{1/2} \quad (29)$$

$\varepsilon_{n1}$ and $\varepsilon_{n2}$ are the roots of, respectively:

$$\varepsilon_{n1}\tan(\varepsilon_{n1}) = \frac{P}{C_{sR}\sigma_1\beta_{w1} + \frac{P}{\gamma_1}} \quad \text{and} \quad (30)$$

$$\varepsilon_{n2}\tan(\varepsilon_{n2}) = \frac{P}{\sigma_2\beta_{w2} + \frac{P}{\gamma_2}}, \quad (31)$$

where $K_0$, $K_1$, $I_0$ and $I_1$ are modified Bessel functions.

## 3. Early time drawdown approximation

Drawdown in phreatic aquifers commonly shows a three-stage profile, i.e., an early, an intermediate and a late stage. The short time approximation of drawdown is briefly summarized below.

The dimensionless time is inversely proportional to the Laplace transform parameter $P$ and small $t$ corresponds to large values of $P$. For this $\varepsilon_{n1}$ and $\varepsilon_{n2}$ approach $(n - 1/2)\pi$, $q_{n1}$ and $q_{n2}$ approach $(C_{sR}P)^{1/2}$ and $(P)^{1/2}$, respectively, and $\sin(\varepsilon_{n1})$ can be approximated by $(-1)^{n-1}$. Then $\bar{s}_{D2}$ given by (24) reduces to

$$\bar{s}_{D2} = \frac{-4K_{rrR}\sqrt{C_{sR}P}K_0(\sqrt{P}r_D)\left[K_0(\sqrt{C_{sR}P}r_{sD})I_1(\sqrt{C_{sR}P}r_{sD}) + I_0(\sqrt{C_{sR}P}r_{sD})K_1(\sqrt{C_{sR}P}r_{sD})\right]}{P[\xi_2\psi_2 - \xi_1\psi_1]} \times \sum_{n=0}^{\infty} \frac{(-1)^{n-1}\cos[(n-0.5)\pi z_D]}{(n-0.5)\pi}, \quad (32)$$

where

$$\xi_1 = \sqrt{C_{sR}P}K_1\left(\sqrt{C_{sR}P}\right) + C_DPK_{rR}K_0\left(\sqrt{C_{sR}P}\right), \quad (33)$$

$$\xi_2 = \sqrt{C_{sR}P}I_1\left(\sqrt{C_{sR}P}\right) - C_DPK_{rR}I_0\left(\sqrt{C_{sR}P}\right), \quad (34)$$

$$\psi_1 = \sqrt{C_{sR}P}K_0\left(\sqrt{P}r_{sD}\right)I_1\left(\sqrt{C_{sR}P}r_{sD}\right) + \sqrt{P}K_{rR}K_1\left(\sqrt{P}r_{sD}\right)I_0\left(\sqrt{C_{sR}P}r_{sD}\right) \quad \text{and} \quad (35)$$

$$\psi_2 = \sqrt{C_{sR}P}K_0\left(\sqrt{P}r_{sD}\right)K_1\left(\sqrt{C_{sR}P}r_{sD}\right) - \sqrt{P}K_{rR}K_0\left(\sqrt{C_{sR}P}r_{sD}\right)K_1\left(\sqrt{P}r_{sD}\right). \quad (36)$$

The summation term in (32) can be calculated by using the following relation [3]:

$$\sum_{n=0}^{\infty}\frac{(-1)^{n-1}\cos[(n-0.5)\pi z_D]}{(n-0.5)\pi}=\begin{cases}\frac{1}{2} & 0\leqslant z_D\leqslant 1\\ 0 & z_D=1\end{cases}. \tag{37}$$

For a large argument $z$, $I_0(z)\to I_1(z)\to e^z/(2\pi z)^{1/2}$, and $K_0(z)\to K_1(z)\to(2\pi z)^{1/2}e^{-z}$ with this approximation, $\bar{s}_{D2}$ can be represented by the following formula

$$\bar{s}_{D2}=\frac{4\sqrt{C_{sR}}\exp\left[-\sqrt{P}\left(r_D-r_{sD}-\sqrt{C_{sR}}+r_{sD}\sqrt{C_{sR}}\right)\right]}{C_DP^2\sqrt{r_D}\left(K_{rR}+\sqrt{C_{sR}}\right)}$$

$$\text{for } r_{sD}>1 \tag{38}$$

$$\bar{s}_{D2}=\frac{2\exp\left[-(-r_D+1)\sqrt{P}\right]}{C_DP^2\sqrt{2-r_D}}\quad \text{for } r_{sD}=1 \tag{39}$$

By performing Laplace inversion the following closed form equations are obtained:

$$s_{D2}=\frac{4\sqrt{C_{sR}}\,\mathrm{erfc}\left[\frac{1}{2\sqrt{t}}\left(r_D-r_{sD}-\sqrt{C_{sR}}+r_{sD}\sqrt{C_{sR}}\right)\right]}{C_D\sqrt{r_D}\left(K_{rR}+\sqrt{C_{sR}}\right)}$$

$$\text{for } r_{sD}>1 \tag{40}$$

$$s_{D2}=\frac{2\,\mathrm{erfc}\left(\frac{-r_D+1}{2\sqrt{t}}\right)}{C_D\sqrt{2-r_D}}\quad \text{for } r_{sD}=1 \tag{41}$$

## 4. Late time drawdown approximation

Large $t$ corresponds to small values of $P$. In this limit, $\varepsilon_{01}$ and $\varepsilon_{02}$ approach $\sqrt{\frac{P}{C_{sR}\sigma_1\beta_{w1}}}$ and $\sqrt{\frac{P}{\sigma_2\beta_{w2}}}$, $q_{01}$ and $q_{02}$ approach $\left(\frac{P}{C_{sR}\sigma_1}+C_{sR}P\right)^{1/2}$ and $\left(\frac{P}{\sigma_2}+P\right)^{1/2}$, respectively, and $\sin(\varepsilon_{01})$ can be approximated by $\varepsilon_{01}$. For $n>0$, $\varepsilon_{n1}$ and $\varepsilon_{n2}$ approach $n\pi$ and $\sqrt{\frac{P}{\sigma_2\beta_{w2}}}$ respectively, $q_{n1}$ and $q_{n2}$ approach $\varepsilon_{n1}\sqrt{\beta_{w1}}$ and $\varepsilon_{n2}\sqrt{\beta_{w2}}$, respectively, and $\sin(\varepsilon_{n1})$ and $\cos(\varepsilon_{n1})$ can be approximated by $\frac{(-1)^nP}{\varepsilon_{n1}C_{sR}\sigma_1\beta_{w1}}$ and $(-1)^n$, respectively. Then $\bar{s}_{D2}$ given by (24) reduces to

$$\bar{s}_{D2}=\frac{-2K_{rR}}{P}\left\{\frac{q_{01}K_0(q_{02}r_D)[K_0(q_{01}r_{sD})I_1(q_{01}r_{sD})+I_0(q_{01}r_{sD})K_1(q_{01}r_{sD})]}{\xi_{02}\psi_{02}-\xi_{01}\psi_{01}}\right.$$
$$\left.+\frac{2P\sqrt{\beta_{w1}}}{C_{sR}\sigma_1\beta_{w1}}\sum_{n=1}^{\infty}\frac{(-1)^n\cos(n\pi z_D)K_0(q_{n2}r_D)[K_0(q_{n1}r_{sD})I_1(q_{n1}r_{sD})+I_0(q_{n1}r_{sD})K_1(q_{n1}r_{sD})]}{n\pi(\xi_{n2}\psi_{n2}-\xi_{n1}\psi_{n1})}\right\}, \tag{42}$$

where

$$\xi_{01}=q_{01}K_1(q_{01})+C_DPK_{rR}K_0(q_{01}), \tag{43}$$
$$\xi_{02}=q_{01}I_1(q_{01})-C_DPK_{rR}I_0(q_{01}), \tag{44}$$
$$\psi_{01}=q_{01}K_0(q_{02}r_{sD})I_1(q_{01}r_{sD})+q_{02}K_{rR}K_1(q_{02}r_{sD})I_0(q_{01}r_{sD}), \tag{45}$$
$$\psi_{02}=q_{01}K_0(q_{02}r_{sD})K_1(q_{01}r_{sD})-q_{02}K_{rR}K_0(q_{01}r_{sD})K_1(q_{02}r_{sD}), \tag{46}$$
$$\xi_{n1}=n\pi\sqrt{\beta_{w1}}K_1(n\pi\sqrt{\beta_{w1}})+C_DPK_{rR}K_0(n\pi\sqrt{\beta_{w1}}), \tag{47}$$
$$\xi_{n2}=n\pi\sqrt{\beta_{w1}}I_1(n\pi\sqrt{\beta_{w1}})-C_DPK_{rR}I_0(n\pi\sqrt{\beta_{w1}})\text{and} \tag{48}$$
$$\psi_{n1}=n\pi\sqrt{\beta_{w1}}K_0(n\pi\sqrt{\beta_{w2}}r_{sD})I_1(n\pi\sqrt{\beta_{w1}}r_{sD})$$
$$+n\pi\sqrt{\beta_{w2}}K_{rR}K_1(n\pi\sqrt{\beta_{w2}}r_{sD})I_0(n\pi\sqrt{\beta_{w1}}r_{sD}). \tag{49}$$

As $P$ is small, the summation term in (38) is negligibly small relative to the first term and the late time drawdown solution can appropriately be described with first term.

For a small argument $z$, $I_0(z)\to 1$, $I_1(z)\to z/2$, $K_0(z)\to -\ln(z)$, $K_1(z)\to 1/z$ and, after the establishment of late time radial flow field, $\bar{s}_{D2}$ can be approximated by the following formula

$$\bar{s}_{D2}=\frac{-2\ln\left(\sqrt{\frac{P}{\sigma_2}+P}r_D\right)}{P}. \tag{50}$$

By performing Laplace inversion the following closed form equation is obtained:

$$s_{D2}=\ln(t)+\gamma-2\ln\left[\sqrt{\frac{(1+\sigma_2)}{\sigma_2}}r_D\right] \tag{51}$$

or

$$s_{D2}=\ln\left[\frac{1.78t\sigma_2}{(1+\sigma_2)r_D^2}\right] \tag{52}$$

where $\gamma=$ Euler's constant (0.5772). The early time solution (Eq. (40)) and the late time solution (Eq. (52)) are compared graphically with the overall response of the phreatic aquifer in the presence of wellbore storage and finite thickness skin (Eq. (24)) in Fig. 3. As can be observed, for $t_D/r_D^2\geqslant 3\times 10^4$ Eq. (47) approximates Eq. (24) and the corresponding curves coincide with each other.

## 5. Results and discussion

To illustrate the effect of the finite thickness skin on the aquifer response, some typical type curves (dimensionless drawdown versus dimensionless time) are plotted using realistic aquifer parameters following Moench [15] ($r_c=r_w=0.1$ m, $b=l=25$ m, $d=0$ (full penetration), $K_{r2}=K_{z2}=10^{-4}$ m s$^{-1}$, $S_{y1}=S_{y2}=0.25$, $S_{s1}=S_{s2}=2\times 10^{-6}$ m$^{-1}$, $\gamma\to\infty$). The influence of skin type, skin thickness, and the contrast of skin hydraulic conductivity relative to the formation hydraulic conductivity, partial penetration, and observation point on expected field results are investigated by generating the type curves in a manner similar to

Novakowski [17]. These type curves may be employed to evaluate the effects of the individual or combination of parameters identical to the field situation.

For the purpose of validating the solution, theoretical responses produced for the case of an infinitesimally thin skin, due to Moench [15], are compared with the solution developed here for the finite thickness skin case (Eq. (24)). The comparison is made between these two solutions for various values of $C_D$ from $10^2$ to $10^6$, at $r_D = 100$, while the skin region is thin ($r_{sD} = 1.1$). Differences are not discernable in the plotted curves (Fig. 2). This comparison suggests that the solution is correct and that the approximation for an infinitesimally thin skin can be used to analyze pumping test results where the skin thickness is very small relative to the radial distance to the observation well. Fig. 3 demonstrates the early time (Eq. (32)) and the late time (Eq. (47)) approximations of Eq. (24). Note that corresponding curves coincide with each other.

We next investigate pumping tests taking into account the influence of a finite thickness skin and wellbore storage effects. A set of type curves were produced with fixed dimensionless parameter values of $K_{rR} = K_{zR} = 100$, $r_D = 100$, and $r_{sD} = 10$ for five successively larger values of $C_D$ in the range 10–$10^5$. This arrangement is equivalent

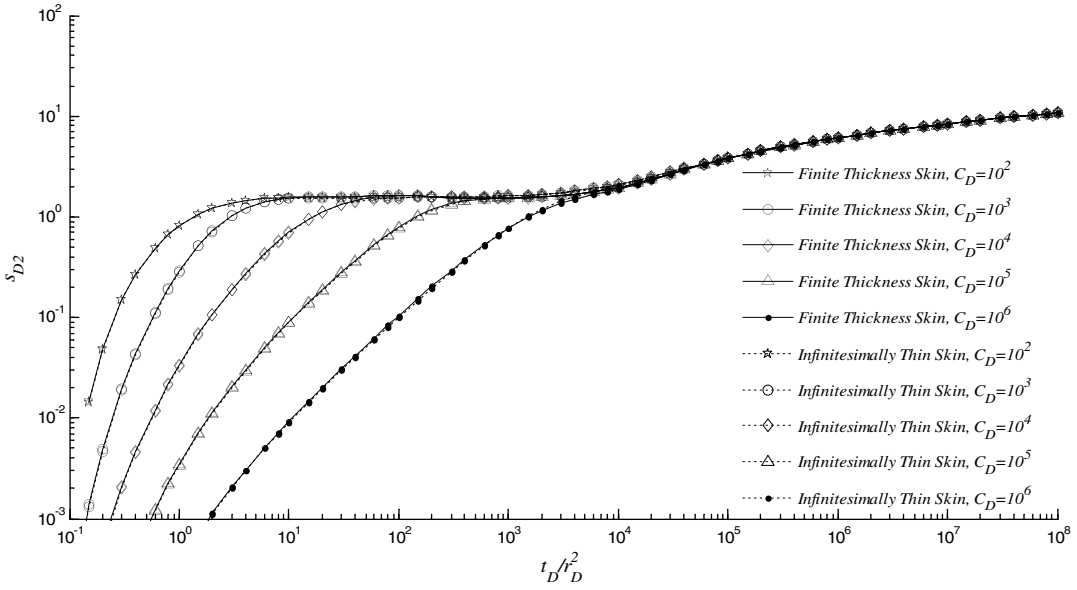


Fig. 2. Comparison of the solution accounting for wellbore storage and infinitesimally thin skin to the solution developed here for the finite thickness skin. In this case $r_{sD} = 1.1$, $K_{rR}$ and $K_{zR} = 100$, $r_D = 100$, with $C_D$ ranging from $10^2$ to $10^6$.

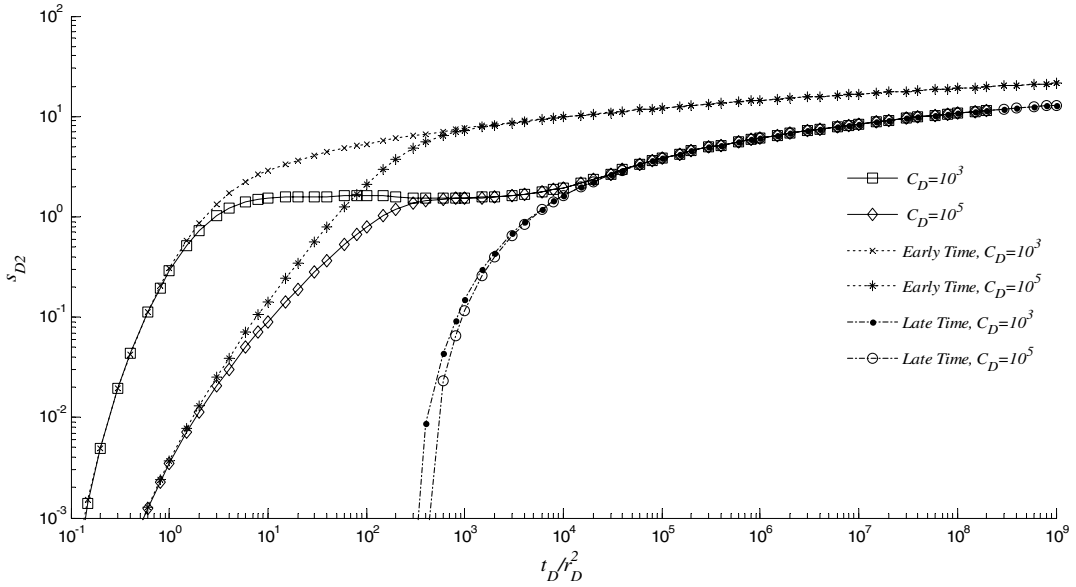


Fig. 3. Comparison of the derived general solution with the early and late time approximations.

to a field setting in which an observation well is 10 m away from a pumping well of 0.1 m radius whose skin region is 1-m thick and has a hydraulic conductivity two orders of magnitude less than that of the formation region. The generated curves are compared with the type curves for an infinitesimally thin skin with $r_{sD} = 1.1$ or $r_s = 0.11$ m (Fig. 4). As can be seen, the skin effects are apparent for the early time segment of the type curves. The effects of increasing skin thickness act to delay the early time drawdown at the observation well. Accurate early time data are needed to characterize the finite thickness skin region. Further, contrary to the confined aquifer [17], the infinitesimally thin skin solution does not approximate the finite thickness solution even in the presence of large wellbore storage.

To examine the phreatic aquifer response to pumping from wells with negative or positive skin, type curves shown in Fig. 5 were generated for $K_{rR} = K_{zR}$ ranging from $10^4$ to $10^{-4}$ at fixed values of $C_D = 10^4$, $r_D = 100$, and $r_{sD} = 10$. $K_{rR} = K_{zR}$ values of $10^4$ to 1 specify positive skin

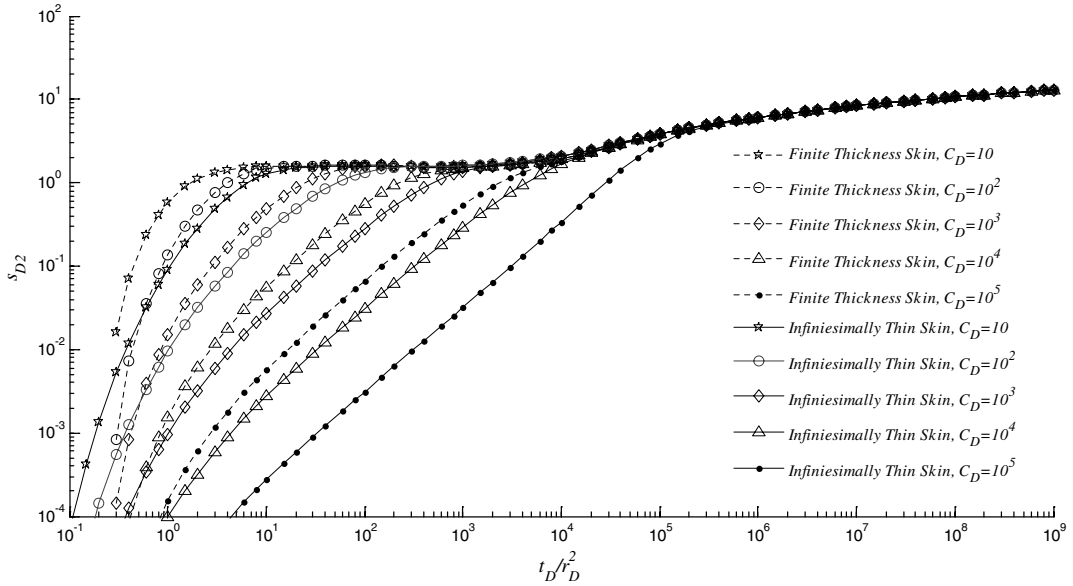


Fig. 4. Comparison of the solution accounting for wellbore storage and infinitesimally thin skin to the solution developed for the finite thickness skin ($K_{rR}$, $K_{zR} = 100$ for $C_D$ ranging from 10 to $10^5$, $r_D = 100$, $r_{sD} = 10$).

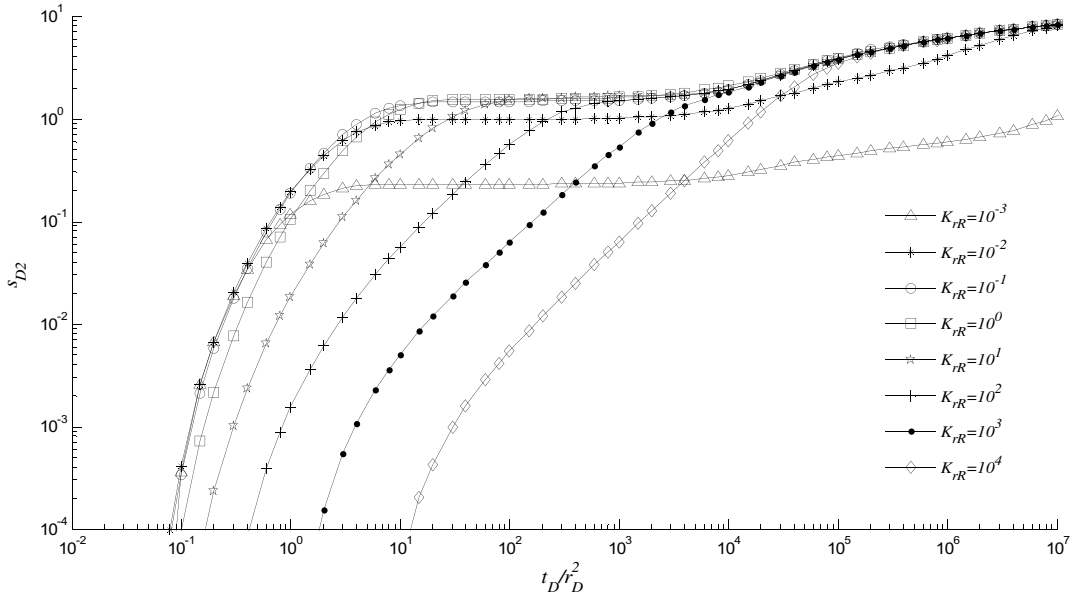


Fig. 5. Type curves developed for the finite thickness skin with various conductivity contrasts between skin and formation ($C_D = 10^4$, $r_D = 100$ and $r_{sD} = 10$, $K_{rR}$ and $K_{zR}$ range from $10^{-3}$ to $10^4$).

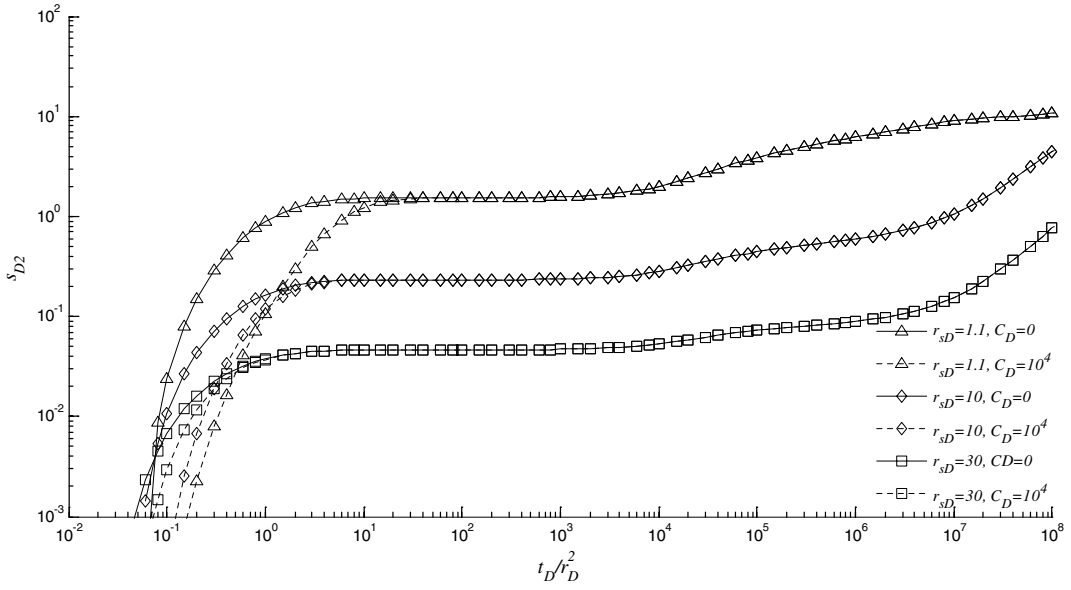


Fig. 6a. Type curves developed for the finite negative skin of different thicknesses ($C_D = 0$ and $10^4$, $r_D = 100$ and, $K_{rR}$, $K_{zR} = 10^{-3}$, $r_{sD} = 1.1$, 10, 30).

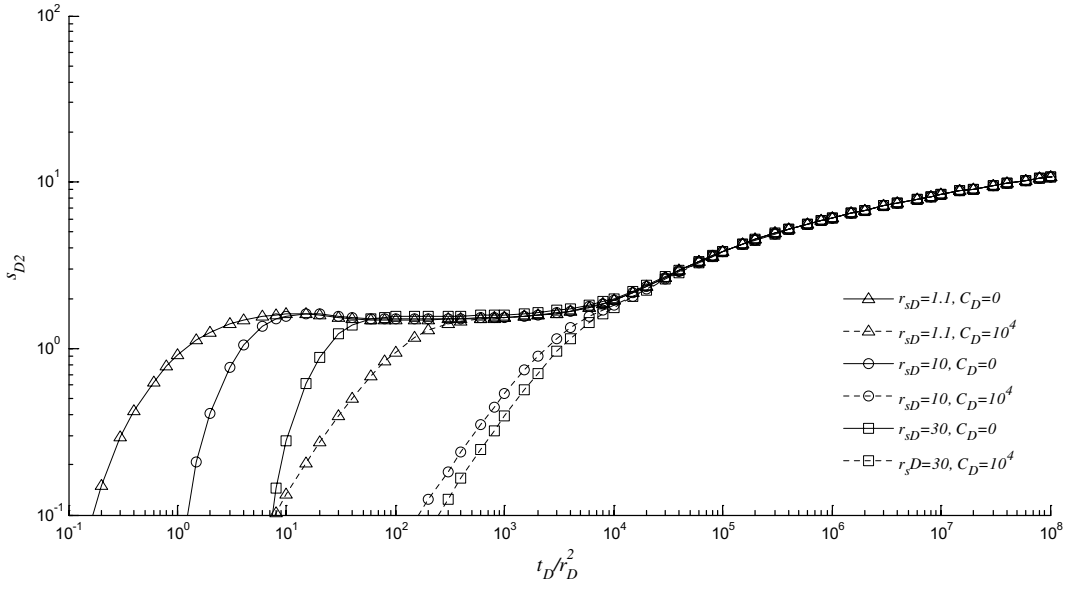


Fig. 6b. Type curves developed for the finite positive skin of different thicknesses ($C_D = 0$ and $10^4$, $r_D$ equals 100 and, $K_{rR}$, $K_{zR}$ $10^3$, $r_{sD}$ of 1.1, 10, 30).

or low permeable skin region relative to the formation region, while values less than 1 define the negative skin or high permeable skin region relative to the formation region. In Fig. 5 two sets of curves are distinguished. One set representing the positive skin and another depicting the negative skin. The effects of positive skin are reflected in the early time segment of the type curves. When an aquifer has a positive skin and is subjected to pumping, the replenishment from the formation is slower so that for successively larger values of $K_{rR} = K_{zR}$ from 1 to $10^4$ the curves are shifted progressively one order of magnitude to the right along the $t_D/r_D^2$ axis. At the intermediate and late time segment of curves, the positive skin effects disappear as all curves coincide and follow the same trend along a common asymptote. In the second set of curves the effects of negative skin are hardly reflected on the early time segment of curves and the position of type curves is rather insensitive to the negative skin. Similar behavior was observed for the case of a confined aquifer [17]. But in contrast to the positive skin, the intermediate and late time segments of the curves, although they follow similar trends, are sharply separated and are highly sensitive to the negative skin. The higher the permeability contrast the higher the separation will be. This behavior is because of the larger permeability and faster replenishment from the formation and also greater effect of delayed drainage.

To explore the phreatic aquifer response to pumping from a well of negative skin of various thicknesses, the

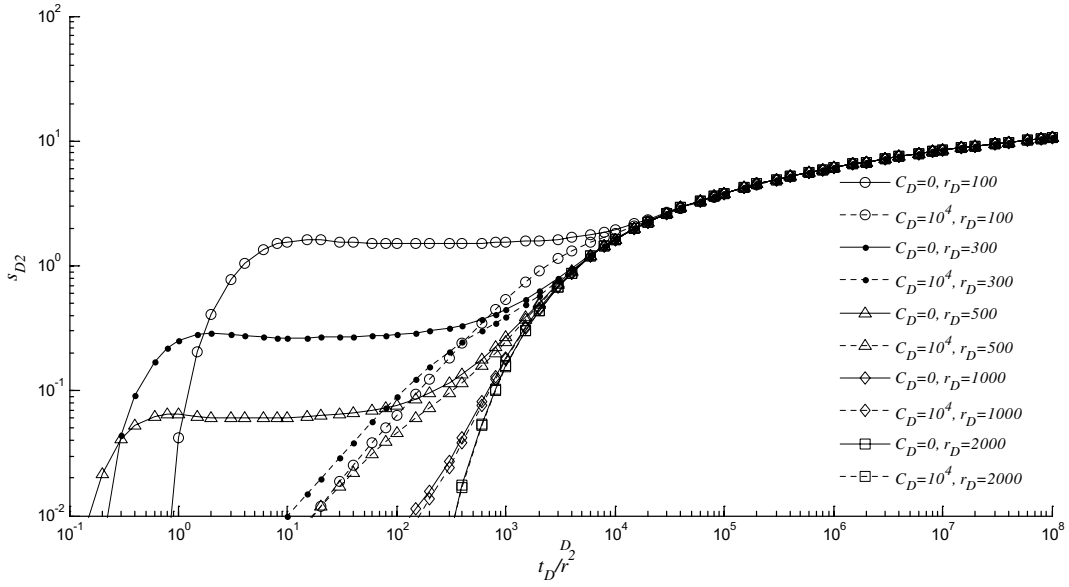


Fig. 7a. Type curves for the positive skin at different observation points ($r_D = 100$, 300, 500, 1000 and 2000, $r_{sD} = 10$, $C_D = 0$ and $10^4$, $K_{rR}$, $K_{zR} = 10^3$).

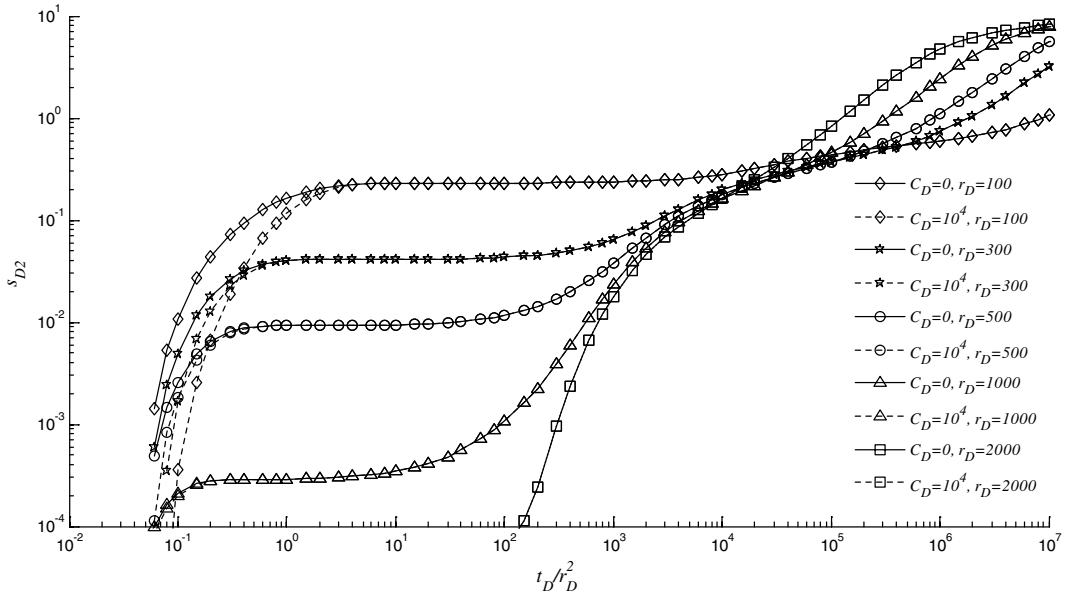


Fig. 7b. Type curves for the negative skin at different observation points ($r_D = 100$, 300, 500, 1000 and 2000, $r_{sD} = 10$, $C_D = 0$ and $10^4$, $K_{rR}$, $K_{zR} = 10^{-3}$).

dimensionless time–drawdown curves illustrated in Fig. 6a were produced for $K_{rR} = K_{zR} = 10^{-3}$, $C_D = 0$ and $10^4$, $r_D = 100$ and $r_{sD} = 1.1$, 10 and 30. While the increase in the wellbore storage shifts the curves to the right less than an order of magnitude as in Fig. 4 and similarly to the confined aquifer [17], the early time segment of the type curves is quite insensitive to the thickness of the negative skin at a fixed value of $C_D$. However, the results for the intermediate and late time segments show differences. At larger $C_D$ the negative skin advances the rate of drawdown at a rather different slope than the case for the smaller $C_D$ and the difference between the time–drawdown curves is more evident. The influence of gradual variation in $r_{sD}$ causes a sharp variation in the intermediate responses. The thicker the negative skin the lower the intermediate and late time drawdown will be. Seemingly, the thicker the negative skin the longer the delayed drainage will persist. This point emphasizes the importance to well development operations in the improvement of permeability contrast in the skin region to enhance the well efficiency. The increase in slope of curves at $t_D/r_D^2 > 10^7$ is due to the low permeability aquifer region relative to high permeable skin, the former tending to behave as a barrier flow boundary.

Fig. 6b is plotted with the same parameter values as Fig. 6a except that the skin is positive with $K_{rR} = K_{zR} = 10^3$. As can be observed, only the early time segment

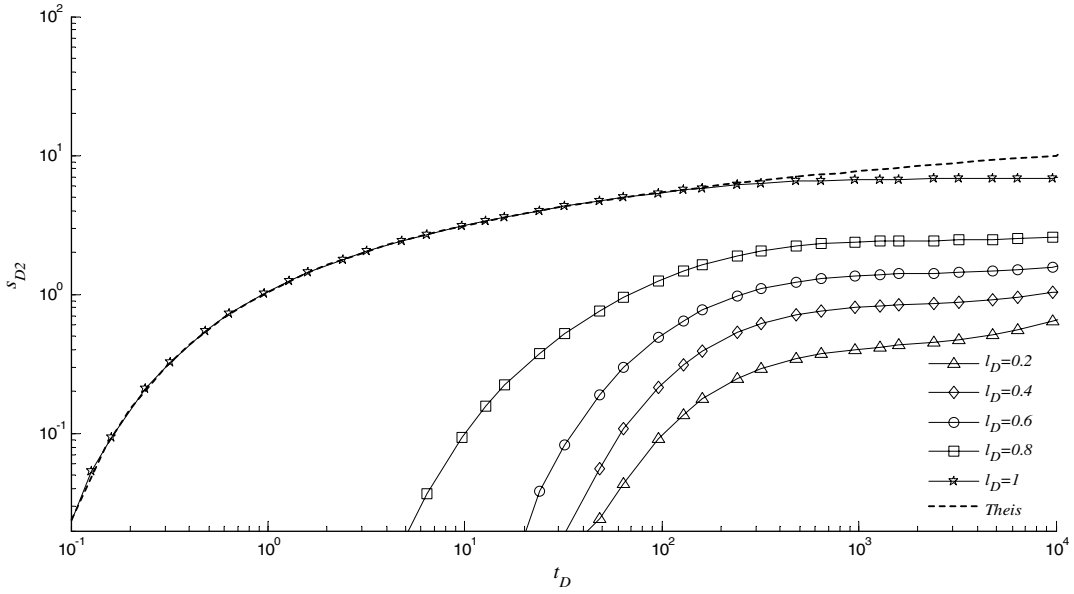


Fig. 8a. The effect of partial penetration for a well of infinitesimal diameter without skin effect based on Neuman [16] ($r_D = 25$, $z_D = 0$, $\sigma_1 = \sigma_2 = 10^{-2}$, $\beta_1 = \beta_2 = 10^{-3}$, $d_D = 0$, $K_{rR}$, $K_{zR} = 1$, $K_{D1} = K_{D2} = 0.1$).

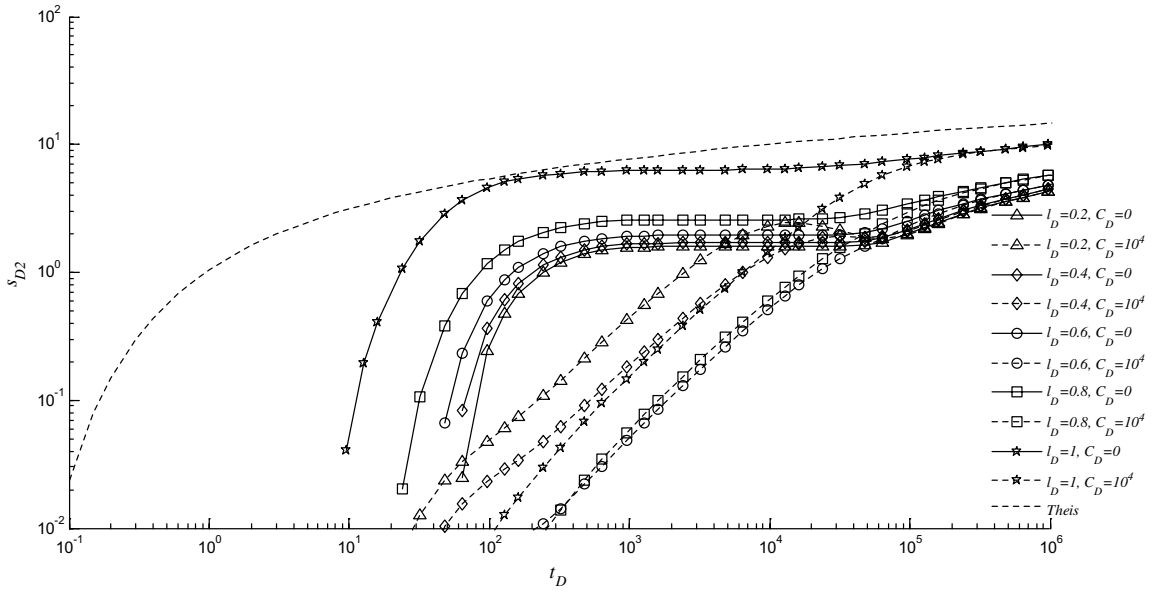


Fig. 8b. The effect of partial penetration for positive skin ($r_D = 25$, $r_{sD} = 10$, $z_D = 0$, $\sigma_1 = \sigma_2 = 10^{-2}$, $\beta_1 = \beta_2 = 10^{-3}$, $d_D = 0$, $C_D = 0$ and $10^4$, $K_{D1} = K_{D2} = 0.1$, $K_{rR}$, $K_{zR} = 10^3$).

of the drawdown curve is affected by the thickness of positive skin and its role is to move the curves to the right. The displacement is over two orders of magnitude for the dimensionless skin thickness of 1.1–30. Note also that again the wellbore storage moves the curves further to the right with flatter slopes and tends to mask the intermediate drawdown or the effect of delayed yield, particularly for the thicker skin. Moreover, for larger wellbore storage the curves are less sensitive to the variations of skin thickness.

To test the influence of positive and negative finite thicknesses skin on the response of the aquifer at various observation points away from the pumped well, e.g., $r_D$ from 100 to 2000, type curves for $C_D$ values of 0 and $10^5$ and $r_{sD} = 10$ are presented in Fig. 7. As for the confined aquifer [17] the influence of the positive finite thickness skin can be identified in a fairly wide range of radial distances from the pumping well. All type curves move towards a common asymptote at large $t_D/r_D^2$ (Fig. 7a). However, the early and intermediate drawdowns reduce at larger $r_D$ so that the effect of the finite skin is diminished. In other words because of extended cone of depression, at large $r_D$ the delayed drainage takes place in an extended area of the formation region and the rate of drawdown decreases. At

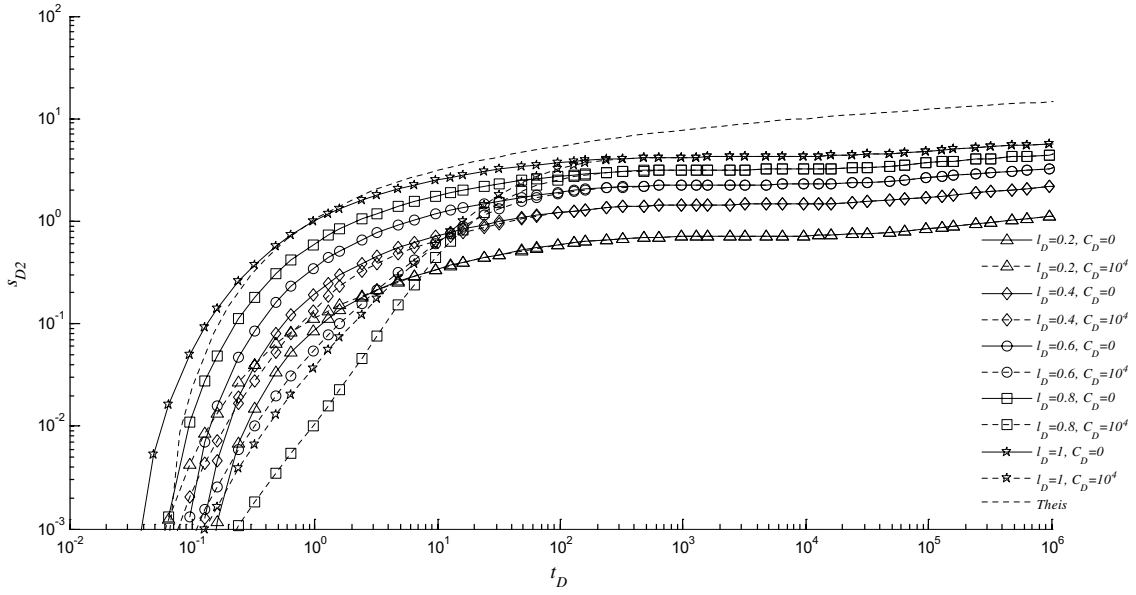


Fig. 8c. The effect of partial penetration for negative skin ($r_D = 25$, $r_{sD} = 10$, $z_D = 0$, $\sigma_1 = \sigma_2 = 10^{-2}$, $\beta_1 = \beta_2 = 10^{-3}$, $d_D = 0$, $C_D = 0$ and $10^4$, $K_{D1} = K_{D2} = 0.1$, $K_{rR}$, $K_{zR} = 10^{-3}$).

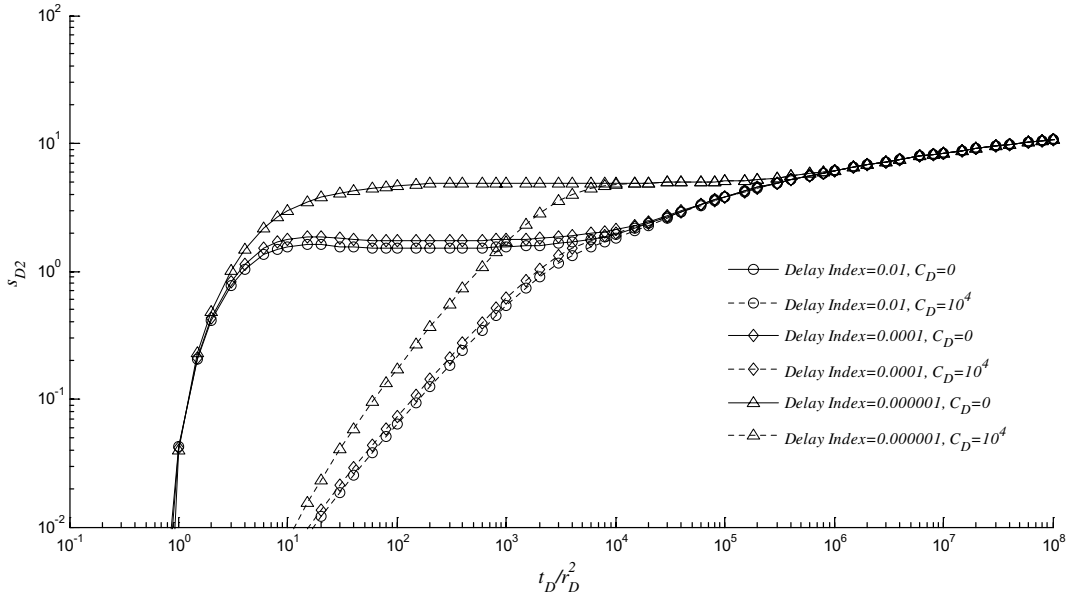


Fig. 9a. The effect of delayed drainage for positive skin ($r_D = 100$, $r_{sD} = 10$, $C_D = 0$ and $10^4$, $K_{rR}$, $K_{zR} = 10^3$).

$r_D = 2000$ the early and intermediate drawdown becomes so small that the corresponding type curve reaches its asymptotic behavior.

In the case of negative skin (Fig. 7b), the permeable skin (in contrast to aquifer permeability) results display the typical behavior of a phreatic aquifer. The less permeable formation region acts the same as a barrier to flow and increases the rate of dimensionless drawdown (from $t_D/r_D^2 = 10^2$ to $t_D/r_D^2 = 10^5$). The influence of the formation region gradually gets more distinct at farther observation points, i.e., from $r_D = 100$ to 2000. Also note that while in Fig. 7a the effect of wellbore storage is well distinguished, in Fig. 7b it is almost masked by the negative skin as demonstrated already in Fig. 5.

Fig. 4 of Neuman [16] is regenerated by our solution (Fig. 8a). This figure illustrates the effects of partial penetration for a phreatic aquifer pumped by a well having no wellbore storage and skin. It is observed that as the well penetrates nearer to the point of observation, an earlier response is observed and the drawdown is greater. Neuman [16] argues that as the depth of penetration (penetration ratio) decreases the importance of gravity effects increases. This increase is of course expected because gravity associated with the vertical component of the flow velocity vector

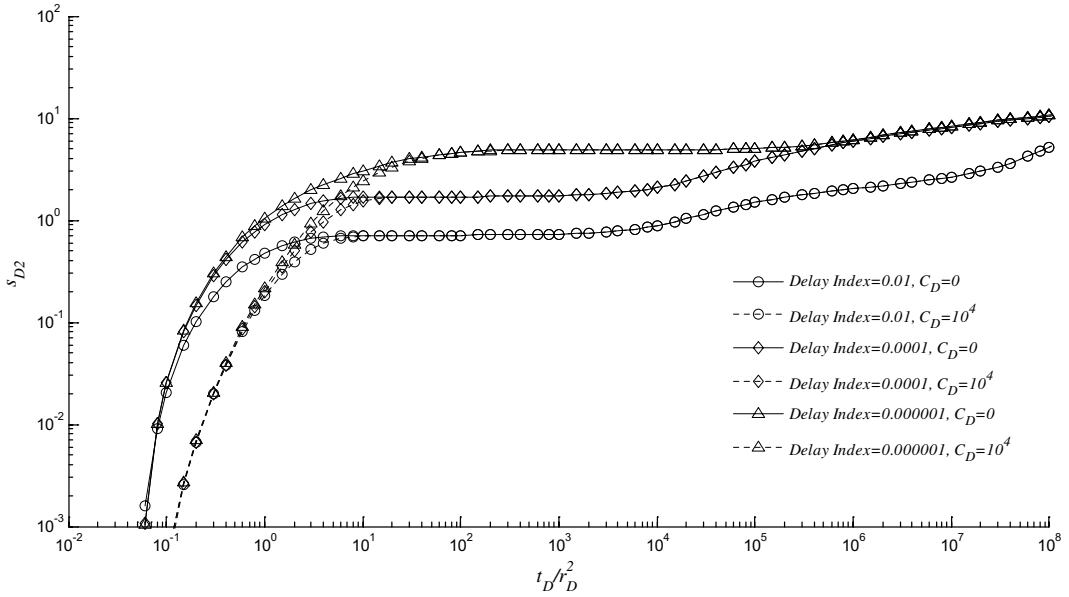


Fig. 9b. The effect of delayed drainage for negative skin ($r_D = 100$, $r_{sD} = 10$, $C_D = 0$ and $10^4$, $K_{rR}$, $K_{zR}$ of $10^{-3}$).

becomes more important when the depth of penetration is small.

To study the effects of partial penetration on the response of the phreatic aquifer pumped by a well of finite thickness skin, type curves shown in Figs. 8b and 8c are plotted for different values of penetration ratios ($l_d$). For the purpose of comparison Figs. 8b and 8c are generated for some parameter values as Fig. 4 in [16], these are $\sigma_1 = \sigma_2 = 10^{-2}$, $\beta_1 = \beta_2 = 10^{-3}$, $d_D = 0$, $K_{D1} = K_{D2} = 0.1$ and the observation point is located at $r_D = 25$ and $z_D = 0$. In these generations wellbore storage and positive/negative skin effect are taken into account. In the case of both positive and negative skins, also a decrease in the penetration ratio causes lower drawdown in the aquifer. In comparison to Fig. 8a, Figs. 8b and 8c demonstrate the same results and indicate that with the presence of either positive or negative skin, the penetration ratio has the same effects on the response of phreatic aquifer when $C_D = 0$, i.e., its decrease delays and decreases the overall drawdown. Fig. 8b further demonstrates that wellbore storage $C_D = 10^4$ delays and decreases the early time drawdown (as expected). However, in contrast to the above arguments, the drawdown decreases as the penetration ratio increases from 0.2 to 0.6 for the case of a positive skin. In other words the gravity flow loses its role in decreasing the drawdown. For the penetration ratio greater than 0.6 the drawdown increases because the depth of penetration is close to the observation point. Note that the above range of penetration ratio values for the negative skin is 0.2–0.8 (Fig. 8c).

For the type curves presented so far, it was assumed that the release of water from the unsaturated zone is instantaneous (delay index $\alpha \to \infty$). Figs. 9a and 9b are plotted to compare the response of the phreatic aquifer pumped by a well of finite thickness skin for various values of $\alpha$ ranging from $10^{-2}$ to $10^{-6}$ for the negative and positive skin, respectively. Higher values of $\alpha$ both for negative and positive skin reduce the early and intermediate drawdowns and the persistence of the intermediate drawdown is increased. The effect for the negative skin is more pronounced. Again the wellbore storage delays and reduces the drawdown as expected.

## 6. Conclusions

A mathematical model is developed for describing the ground water flow in phreatic aquifers with two regions of radial flow in response to a constant rate pumping test. The model incorporates the effects of partial penetration, well storage, anisotropy, finite radius well skin and non-instantaneous release of water from the unsaturated zone. The solution is first derived using Laplace transforms. Time-domain solutions of dimensionless drawdown–time-time curves were then obtained from the numerical inversion of the Laplace transforms. This solution can be used either to predict the drawdown or to investigate the effects of the wellbore storage, skin type, skin thickness, and the permeability contrast between skin and formation region on drawdown distribution at the pumping well as well as any observation point in the skin and formation regions. The interpretation of the type curves leads to the following conclusions:

- The infinitesimally thin skin solution developed by Moench [15] can approximate the developed finite thickness skin solution where the skin region is thin. When the skin region is thick the infinitesimally thin skin solution can never approximate the developed finite skin solution even for large wellbore storage.
- The positive skin effects are reflected in the early time results and disappear in the intermediate and late time

aquifer responses. The negative skin effects are however disguised at the early time and manifested at the intermediate and late time aquifer responses. In general the higher the permeability contrast between skin and formation the higher the deviation from the uniform solution.

- The thick negative skin lowers the overall drawdown in the aquifer and causes the delayed drainage to persist longer. This highlights the importance of well development operations. The time–drawdown curve of an aquifer pumped by a well of thick negative skin shows the typical behavior of a phreatic aquifer affected by a barrier flow boundary. The thicker the skin the sharper the effect of the boundary. In general the negative skin tends to disguise the wellbore storage effect. The thick positive skin delays the early time drawdown and shortens the intermediate time response.
- The observation point distance from the pumping well with finite skin has a pronounced effect on the time–drawdown curves. For the negative skin the formation region acts as a barrier flow boundary. At distant observation points the effects of a positive skin are too small to be reflected on the early and intermediate aquifer responses and the type curve takes its asymptotic form.
- Partial penetration decreases the drawdown in the case of both positive and negative skin; however this effect may be reversed in the presence of wellbore storage for some particular range of penetration ratio.
- An increase in delayed drainage for negative and positive skin reduces the early and intermediate drawdowns and causes an increased persistence of intermediate drawdown. This effect is more pronounced for the negative skin.

## Acknowledgement

Financial support provided by the Ministry of Science, Research and Technology of Iran, Shiraz University and EPFL, Switzerland for the first author are acknowledged.

## Appendix. Analytical solution

The governing equations in dimensionless format are

$$\frac{\partial^2 s_{D1}}{\partial r_D^2}+\frac{1}{r_D}\frac{\partial s_{D1}}{\partial r_D}+\beta_{w1}\frac{\partial^2 s_{D1}}{\partial z_D^2}=C_{sR}\frac{\partial s_{D1}}{\partial t_D},\quad 1\leqslant r_D\leqslant r_{sD}, \tag{A1}$$

$$\frac{\partial^2 s_{D2}}{\partial r_D^2}+\frac{1}{r_D}\frac{\partial s_{D2}}{\partial r_D}+\beta_{w2}\frac{\partial^2 s_{D2}}{\partial z_D^2}=\frac{\partial s_{D2}}{\partial t_D},\quad r_D\geqslant r_{sD}. \tag{A2}$$

For the definition of the dimensionless parameters refer to Table 1. The associated dimensionless inner and outer boundary conditions are given by

$$s_{D1}(r_D,z_D,0)=s_{D2}(r_D,z_D,0)=0, \tag{A3}$$

$$s_{wD}(r_{wD},z_D,0)=0, \tag{A4}$$

$$s_{D2}(\infty,z_D,t_D)=0, \tag{A5}$$

$$\left.\frac{\partial s_{D1}}{\partial r_D}\right|_{r_D=1}=0,\quad z_D<1-l_D, z_D>1-d_D, \tag{A6}$$

$$\left.\frac{\partial s_{D1}}{\partial r_D}\right|_{r_D=1}=K_{rR}\left(C_D\frac{\mathrm{d}s_{wD}}{\mathrm{d}t_D}-\frac{2}{l_D-d_D}\right),\quad 1-l_D\leqslant z_D\leqslant 1-d_D, \tag{A7}$$

$$\left.\frac{\partial s_{D1}}{\partial z_D}\right|_{z_D=0}=\left.\frac{\partial s_{D2}}{\partial z_D}\right|_{z_D=0}=0, \tag{A8}$$

$$\left.\frac{\partial s_{D1}}{\partial z_D}\right|_{z_D=1}=-\gamma_1\int_0^{t_D}\frac{\partial s_{D1}}{\partial t'_D}\mathrm{e}^{-C_{sR}\gamma_1\sigma_1\beta_{w1}(t_D-t'_D)}\,\mathrm{d}t'_D,\quad 1\leqslant r_D\leqslant r_{sD}, \tag{A9}$$

$$\left.\frac{\partial s_{D2}}{\partial z_D}\right|_{z_D=1}=-\gamma_2\int_0^{t_D}\frac{\partial s_{D2}}{\partial t'_D}\mathrm{e}^{-\gamma_2\sigma_2\beta_{w2}(t_D-t'_D)}\mathrm{d}t'_D,\quad r_D\geqslant r_{sD}, \tag{A10}$$

$$s_{wD}(1,z_D,t_D)=s_{D1}(1,z_D,t_D), \tag{A11}$$

$$s_{D1}(r_{sD},z_D,t_D)=s_{D2}(r_{sD},z_D,t_D)\quad\text{and} \tag{A12}$$

$$\frac{\partial s_{D1}(r_{sD},z_D,t_D)}{\partial r_D}=K_{rR}\frac{\partial s_{D2}(r_{sD},z_D,t_D)}{\partial r_D}. \tag{A13}$$

The solution for the dimensionless drawdowns in both the skin and formation zones can be obtained by taking Laplace transforms of Eqs. (A1)–(A3).

$$\frac{\partial^2 \bar{s}_{D1}}{\partial r_D^2}+\frac{1}{r_D}\frac{\partial \bar{s}_{D1}}{\partial r_D}+\beta_{w1}\frac{\partial^2 \bar{s}_{D1}}{\partial z_D^2}=C_{sR}P\bar{s}_{D1},\quad 1\leqslant r_D\leqslant r_{sD}, \tag{A14}$$

$$\frac{\partial^2 \bar{s}_{D2}}{\partial r_D^2}+\frac{1}{r_D}\frac{\partial \bar{s}_{D2}}{\partial r_D}+\beta_{w2}\frac{\partial^2 \bar{s}_{D2}}{\partial z_D^2}=P\bar{s}_{D2},\quad r_D\geqslant r_{sD}, \tag{A15}$$

$$\bar{s}_{D2}(\infty,z_D,P)=0, \tag{A16}$$

$$\left.\frac{\partial s_{D1}}{\partial r_D}\right|_{r_D=1}=0,\quad \text{for } z_D<1-l_D, z_D>1-d_D, \tag{A17}$$

$$\left.\frac{\mathrm{d}\bar{s}_{D1}}{\mathrm{d}r_D}\right|_{r_D=1}=K_{rR}\left(C_DP\bar{s}_{wD}-\frac{2}{P(l_D-d_D)}\right),\quad 1-l_D\leqslant z_D\leqslant 1-d_D, \tag{A18}$$

$$\left.\frac{\partial \bar{s}_{D1}}{\partial z_D}\right|_{z_D=0}=\left.\frac{\partial \bar{s}_{D2}}{\partial z_D}\right|_{z_D=0}=0, \tag{A19}$$

$$\left.\frac{\partial \bar{s}_{D1}}{\partial z_D}\right|_{z_D=1}=-\frac{P\bar{s}_{D1}}{C_{sR}\sigma_1\beta_{w1}+\frac{P}{\gamma_1}},\quad 1\leqslant r_D\leqslant r_{sD}, \tag{A20}$$

$$\left.\frac{\partial \bar{s}_{D2}}{\partial z_D}\right|_{z_D=1}=-\frac{P\bar{s}_{D2}}{\sigma_2\beta_{w2}+\frac{P}{\gamma_2}},\quad r_D\geqslant r_{sD}, \tag{A21}$$

$$\bar{s}_{wD}(1,z_D,P)=\bar{s}_{D1}(1,z_D,P), \tag{A22}$$

$$\bar{s}_{D1}(r_{sD},z_D,P)=\bar{s}_{D2}(r_{sD},z_D,P)\quad\text{and} \tag{A23}$$

$$\frac{\partial \bar{s}_{D1}(r_{sD},z_D,P)}{\partial r_D}=K_{rR}\frac{\partial \bar{s}_{D2}(r_{sD},z_D,P)}{\partial r_D}. \tag{A24}$$

Solutions to (A14) and (A15) that satisfy (A19)–(A21) are

$$\bar{s}_{D1}=\sum_{n=0}^{\infty}\bar{f}_{n1}(r_D,P)\cos(\varepsilon_{n1}z_D)\quad\text{and} \tag{A25}$$

$$\bar{s}_{D2}=\sum_{n=0}^{\infty}\bar{f}_{n2}(r_D,P)\cos(\varepsilon_{n2}z_D), \tag{A26}$$

where $\varepsilon_{n1}$ and $\varepsilon_{n2}$ are the roots of

$$\varepsilon_{n1}\tan(\varepsilon_{n1}) = \frac{P}{C_{sR}\sigma_1\beta_{w1} + \frac{P}{\gamma_1}} \quad \text{and} \quad \varepsilon_{n2}\tan(\varepsilon_{n2}) = \frac{P}{\sigma_2\beta_{w2} + \frac{P}{\gamma_2}}. \tag{A27}$$

Substitution of (A25) and (A26) into (A14) and (A15) yields

$$\sum_{n=0}^{\infty}\left\{\frac{\partial^2\bar{f}_{n1}(r_D,P)}{\partial r_D^2} + \frac{1}{r_D}\frac{\partial\bar{f}_{n1}(r_D,P)}{\partial r_D} - [\beta_{w1}\varepsilon_{n1}^2 + C_{sR}P]\bar{f}_{n1}(r_D,P)\right\}\cos(\varepsilon_{n1}z_D) = 0 \quad \text{and} \tag{A28}$$

$$\sum_{n=0}^{\infty}\left[\frac{\partial^2\bar{f}_{n2}(r_D,P)}{\partial r_D^2} + \frac{1}{r_D}\frac{\partial\bar{f}_{n2}(r_D,P)}{\partial r_D} - (\beta_{w2}\varepsilon_{n2}^2 + P)\bar{f}_{n2}(r_D,P)\right]\cos(\varepsilon_{n2}z_D) = 0. \tag{A29}$$

Hence $f_{n1}$ and $f_{n2}$ must satisfy

$$\frac{\partial^2\bar{f}_{n1}(r_D,P)}{\partial r_D^2} + \frac{1}{r_D}\frac{\partial\bar{f}_{n1}(r_D,P)}{\partial r_D} - [\beta_{w1}\varepsilon_{n1}^2 + C_{sR}P]\bar{f}_{n1}(r_D,P) = 0 \quad \text{and} \tag{A30}$$

$$\frac{\partial^2\bar{f}_{n2}(r_D,P)}{\partial r_D^2} + \frac{1}{r_D}\frac{\partial\bar{f}_{n2}(r_D,P)}{\partial r_D} - (\beta_{w2}\varepsilon_{n2}^2 + P)\bar{f}_{n2}(r_D,P) = 0. \tag{A31}$$

The general solution of (A30) is

$$\bar{f}_{n1}(r_D,P) = g_n(P)K_0(q_{n1}r_D) + w_n(P)I_0(q_{n1}r_D) \tag{A32}$$

and because of (A16), the general solution of (A30) is

$$\bar{f}_{n2}(r_D,P) = u_n(P)K_0(q_{n2}r_D). \tag{A33}$$

Substitution of (A32) and (A33) to (A25) and (A26) yields

$$\bar{s}_{D1} = \sum_{n=0}^{\infty}[g_n(P)K_0(q_{n1}r_D) + w_n(P)I_0(q_{n1}r_D)]\cos(\varepsilon_{n1}z_D) \quad \text{and} \tag{A34}$$

$$\bar{s}_{D2} = \sum_{n=0}^{\infty}u_n(P)K_0(q_{n2}r_D)\cos(\varepsilon_{n2}z_D), \tag{A35}$$

where $q_{n1} = (\beta_{w1}\varepsilon_{n1}^2 + C_{sR}P)^{1/2}$, $q_{n2} = (\beta_{w2}\varepsilon_{n2}^2 + P)^{1/2}$ and $K_0$ and $I_0$ are the zero-order modified Bessel functions of the second and first kind, respectively, and $g_n$, $w_n$ and $u_n$ are coefficients to be determined.

If the boundary condition (A23) is employed

$$[g_n(P)K_0(q_{n1}r_{sD}) + w_n(P)I_0(q_{n1}r_{sD})]\cos(\varepsilon_{n1}z_D) = u_n(P)K_0(q_{n2}r_{sD})\cos(\varepsilon_{n2}z_D). \tag{A36}$$

Boundary condition (A24) gives

$$[w_n(P)q_{n1}I_1(q_{n1}r_{sD}) - g_n(P)q_{n1}K_1(q_{n1}r_{sD})]\cos(\varepsilon_{n1}z_D) = K_{rR}[-u_n(P)q_{n2}K_1(q_{n2}r_{sD})]\cos(\varepsilon_{n2}z_D). \tag{A37}$$

Substituting (A34) into (A18) and letting the substitution of $\bar{s}_{wD}$ based on (A22) yields

$$\sum_{n=0}^{\infty}[w_n(P)q_{n1}I_1(q_{n1}) - g_n(P)q_{n1}K_1(q_{n1})]\cos(\varepsilon_{n1}z_D) = C_DPK_{rR}\sum_{n=0}^{\infty}[w_n(P)I_0(q_{n1}) + g_n(P)K_0(q_{n1})]\times\cos(\varepsilon_{n1}z_D) - \frac{2K_{rR}}{P(l_D-d_D)}. \tag{A38}$$

Applying (A17) one obtains

$$\sum_{n=0}^{\infty}[w_n(P)q_{n1}I_1(q_{n1}) - g_n(P)q_{n1}K_1(q_{n1})]\cos(\varepsilon_{n1}z_D) = 0. \tag{A39}$$

Multiplying (A38) by $\cos(\varepsilon_{m1}z_D)$ and integrating over the indicated interval, one obtains

$$\sum_{n=0}^{\infty}[w_n(P)q_{n1}I_1(q_{n1}) - g_n(P)q_{n1}K_1(q_{n1})]\int_{1-l_D}^{1-d_D}\times\cos(\varepsilon_{n1}z_D)\cos(\varepsilon_{m1}z_D)\mathrm{d}z_D = C_DPK_{rR}\sum_{n=0}^{\infty}[w_n(P)I_0(q_{n1}) + g_n(P)K_0(q_{n1})]\int_{1-l_D}^{1-d_D}\cos(\varepsilon_{n1}z_D)\cos(\varepsilon_{m1}z_D)\mathrm{d}z_D - \frac{2K_{rR}}{P(l_D-d_D)}. \tag{A40}$$

Multiplying (A39) by $\cos(\varepsilon_{m1}z_D)$ and integrating over the below and above the screen, one obtains

$$\sum_{n=0}^{\infty}[w_n(P)q_{n1}I_1(q_{n1}) - g_n(P)q_{n1}K_1(q_{n1})]\times\int_0^{1-l_D}\cos(\varepsilon_{n1}z_D)\cos(\varepsilon_{m1}z_D) = 0 \quad \text{and} \tag{A41}$$

$$\sum_{n=0}^{\infty}[w_n(P)q_{n1}I_1(q_{n1}) - g_n(P)q_{n1}K_1(q_{n1})]\times\int_{1-d_D}^{0}\cos(\varepsilon_{n1}z_D)\cos(\varepsilon_{m1}z_D) = 0. \tag{A42}$$

Adding (A41) and (A42) to the left-hand side of (A40) and considering that all terms in the sum on the left-hand side of the result are zero except those for which $n = m$, the set $\cos(\varepsilon_{n1}z_D)$ is orthogonal over the interval 0, 1 and so one obtains

$$[w_n(P)q_{n1}I_1(q_{n1}) - g_n(P)q_{n1}K_1(q_{n1})]\int_0^1\cos^2(\varepsilon_{n1}z_D)\,\mathrm{d}z_D = C_DPK_{rR}[w_n(P)I_0(q_{n1}) + g_n(P)K_0(q_{n1})]\times\int_{1-l_D}^{1-d_D}\cos^2(\varepsilon_{n1}z_D)dz_D - \frac{2K_{rR}}{P(l_D-d_D)}\times\int_{1-l_D}^{1-d_D}\cos(\varepsilon_{n1}z_D)\,\mathrm{d}z_D. \tag{A43}$$

The Eqs. (A36), (A37) and (A42) can be solved to determine the constants $g_n$, $w_n$ and $u_n$ which are then substituted into (A34) and (A35) to obtain the solutions for $\bar{s}_{D1}$ and. $\bar{s}_{D2}$, respectively.

## References


[1] Boulton NS. Analysis of data from non-equilibrium pumping tests allowing for delayed yield from storage. Proc Inst Civil Eng 1963;26:469–82.

[2] Butler JJ. Pumping tests in nonuniform aquifers-the radially symmetric case. J Hydrol 1988;101:15–30.

[3] Chen CS, Chang CC. Theoretical well hydraulics theory and data analysis for the constant head test in an unconfined aquifer with skin effect. Water Resour Res 2003;39(6):1121. doi:10.1029/2002WR001516.

[4] Chen CS, Chang CC. Theoretical evaluation of non-uniform skin effect on aquifer response under constant rate pumping. J Hydrol 2006;317:190–201.

[5] Chu WC, Garcia-Rivera J, Raghaven R. Analysis of interference test data influenced by wellbore storage and skin at the flowing well. J Pet Technol 1980;32:263–9.

[6] Cimen M. Type curves for unsteady flow to a large-diameter well in Patchy aquifer. J Hydraul Eng 2005;10(3):200–4.

[7] Dougherty DE, Babu DK. Flow to a partially penetrating well in a double-porosity reservoir. Water Resour Res 1984;20(8):1116–22.

[8] Earlougher Jr RC. Advances in well test analysis. Monogr. Ser, vol. 5. Dallas: Society of Petroleum Engineers; 1977.

[9] Hantush MS. Hydraulics of wells. Advances in hydroscience, vol. 1. California, San Diego: Academic; 1964. p. 281–432.

[10] Hawkins Jr MF. A note on the skin effect. Trans Am Inst Min Metal Pet Eng 1956;207:356–67.

[11] Karasaki K. Well test analysis in fractured media. PhD thesis, University of California, Berkeley; 1986.

[12] Markle JM, Rowe RK, Novakowski KS. A model for the constant-head pumping test conducted in vertically fractured media. Int J Numer Anal Meth Geomech 1995;19:457–73.

[13] Moench AF. Transient flow to a large-diameter well in an aquifer with storative semiconfining layers. Water Resour Res 1985;21(8):1121–31.

[14] Moench AF, Hsieh PA. Analysis of slug test data in a well with finite thickness skin. In: Proceedings of the 17th international congress, Int Assoc Hydrogeol, Tucson, Ariz; 1985.

[15] Moench AF. Flow to a well of finite diameter in a homogeneous, anisotropic phreatic aquifer. Water Resour Res 1997;33(6):1397–407.

[16] Neuman SP. Effects of partial penetration on flow in unconfined aquifers considering delayed aquifer response. Water Resour Res 1974;10(2):303–12.

[17] Novakowski KS. A composite analytical model for analysis of pumping tests affected by well bore storage and finite thickness skin. Water Resour Res 1989;25(9):1937–46.

[18] Novakowski KS. Interpretation of the transient flow rate obtained from constant-head tests conducted in situ in clays. Can Geotech J 1993;30:600–6.

[19] Ogbe DO, Brigham WE. A model for interference testing with wellbore storage and skin effects at both wells. In: Proceedings of the 59th annual technical conference, Soc Pet Eng, Houston, TX; 1984.

[20] Papadopoulos IS, Cooper Jr HH. Drawdown in a well of large diameter. Water Resour Res 1967;3(1):241–4.

[21] Park E, Zhan H. Hydraulics of a finite-diameter horizontal well with wellbore storage and skin effect. Adv Water Resour 2002;25(4):389–400.

[22] Park E, Zhan H. Hydraulics of horizontal wells in fractured shallow aquifer systems. J Hydrol 2003;281:147–58.

[23] Perina T, Lee TC. General well function for pumping from a confined, leaky, or unconfined aquifer. J Hydrol 2006;317:239–60.

[24] Ramey Jr HJ, Agarwal RG. Annulus unloading rates and wellbore storage. Soc Pet Eng J 1972;24:453–62.

[25] Sandal HM, Horne RN, Ramey HJ, Williamson JW. Interference testing with wellbore storage and skin effects at the produced well. In: Proceedings of the 53rd annual technical conference, Soc Pet Eng, Houston, TX; 1978.

[26] Stehfest H. Numerical inversion of Laplace transforms. Commun ACM 1970;13(1):47–9.

[27] Tongpenyai Y, Raghaven R. The effect of wellbore storage and skin on interference test data. J Pet Technol 1981;33:151–60.

[28] Van Everdingen AF, Hurst W. The application of the Laplace transformation to flow problems in reservoirs. Trans Am Inst Min Metall Pet Eng 1949;186:305–24.

[29] Wang JSY, Narasimhan TN, Tsang CF, Witherspoon PA, Transient flow in tight fractures. Report LBL-7027, Lawrence Berkeley Lab, Berkeley, CA; 1978. p. 103–16.

[30] Yang SY, Yeh HD. Laplace-domain solutions for radial two-zone flow equations under the conditions of constant-head and partially well. J Hydraul Eng 2005;131(3):209–15.

[31] Yang SY, Yeh HD. Solution for flow across the wellbore in a two-zone confined aquifer. J Hydraul Eng 2002;128(2):175–83.

[32] Yeh HD, Yang SY, Peng HY. A new closed-form solution for a radial two-layer drawdown equation for groundwater under constant-flux pumping in a finite-radius well. Adv Water Resour 2003;26:747–57.

[33] Yeh HD, Yang SY. A novel analytical solution for a slug test conducted in a well with a finite-thickness skin. Adv Water Resour 2006;29(10):1479–89.